

# 변단면 수평 곡선보의 자유진동에 관한 연구

## Free Vibrations of Horizontally Curved Beams with Variable Cross Section

이 병 구\*    박 광 규\*\*    모 정 만\*\*\*    이 재 만\*\*\*  
Lee, Byoung-Koo    Park, Kwang-Kyou    Mo, Jeong-Man    Lee, Jae-Man

### 요 지

이 논문은 변단면을 고려한 수평 곡선보의 자유진동에 관한 연구이다. 진동시 곡선보 요소에 작용하는 합응력과 관성력의 동적평형방정식을 이용하여 변단면 원호형 수평 곡선보의 자유진동을 지배하는 상미분방정식을 유도하였다. 이 미분방정식을 원형 단면을 갖는 선형변단면에 적용하여 고유진동수, 진동형 및 합응력을 산출하였다. 수치 해석에에서는 양단고정 및 양단회전 곡선보를 채택하였으며, 수치해석 결과로서 고유진동수와 단면비, 세장비 및 중심각 사이의 관계를 그림에 나타내었다. 또한 실험실 규모의 실험을 통하여 본 연구결과의 타당성을 보였다.

핵심용어 : 면외진동, 변단면, 선형변단면, 수평곡선보, 실험측정, 진동형, 합응력

### Abstract

The differential equations governing free, out-of-plane vibrations of horizontally circular curved beams with variable cross-section are derived and solved numerically for linear tapers with circular cross-section. In the numerical methods, the Runge-Kutta and Determinant Search methods are used for computing the natural frequencies and mode shapes. Experimental measurements of frequencies agree closely with those predicted by theory. Frequencies, mode shapes and cross-sectional stress resultants are reported. The numerical methods here for computing frequencies and mode shapes are efficient and reliable.

*Keywords* : experimental measurement, horizontally curved beam, linear taper, mode shape, out-of-plane vibration, stress resultants, variable cross-section

## 1. INTRODUCTION

Studies on the free vibrations of linearly elastic curved beams of various geometries

have been reported by many investigators. Such studies were critically reviewed by Wang, et al.<sup>1)</sup> and Lee and Wilson<sup>2)</sup>.

Briefly, the exact solutions of such works

\* 정회원·원광대학교 토목환경공학과, 교수  
\*\* 정회원·대전대학교 토목공학과, 교수  
\*\*\* 정회원·원광대학교 토목환경공학과, 대학원

• 이 논문에 대한 토론을 1998년 12월 31일까지 본 학회에 보내주시면 1999년 3월호에 그 결과를 게재하겠습니다.

included studies with prediction of the frequencies in extension by Archer<sup>3)</sup>, in flexure with symmetric and anti-symmetric modes by Morley<sup>4)</sup> and in coupled twist-bending by Ojalvo<sup>5)</sup>.

Approximate methods have been developed in calculating the natural frequencies of curved beams. Such works using the Rayleigh-Ritz method included studies by Den Hartog<sup>6)</sup>, Volterra and Morell<sup>7)</sup>, Nelson<sup>8)</sup> and Wang and Lee<sup>9)</sup>.

Additional research in the field of bridge structures included the investigations by Yonezawa<sup>10)</sup> and Tan and Shore<sup>11)</sup>. Also, the works with the Timoshenko theory which includes the effects of rotatory inertia and shear deformation in the free vibrations have done by Rao and Sundararajan<sup>12)</sup>, Philipson<sup>13)</sup> and Seidel and Erdelyi<sup>14)</sup>.

In the open literature, the works on the free vibration of horizontally curved beam with variable cross-section are very rare. The main purpose of the present paper is, therefore, to present a numerical method for calculating the natural frequencies and mode shapes of such curved beams.

Differential equations were derived for out-of-plane free vibration of linearly elastic circular curved beam with variable cross-section. Although the effects of structural damping and warping were neglected, the effects of rotatory inertia and shear deformation were included i. e. the Timoshenko theory was considered in the governing equations. And it is assumed that the elastic center, shear center and the center of twist of the cross-section are coincident.

The linear taper with circular cross-section was used as the shape functions of the variable cross-section. The governing differential equations were solved numerically to obtain the

frequencies and mode shapes. In numerical examples, the curved beams with both clamped ends and both hinged ends were considered. The four lowest natural frequencies are presented as functions of three non-dimensional system parameters: section ratio, slenderness ratio and opening angle. Also, the mode shapes of displacements and stress resultants are shown in figures. In addition, the free vibration frequencies of two laboratory-scale curved beams were measured; and these results agree quite well with the present numerical studies.

## 2. MATHEMATICAL MODEL

The geometry of circular curved beam with variable cross-section, symmetric about the mid span, is defined in Figure 1(a). Both ends are either clamped or hinged. Its radius and opening angle are  $a$  and  $\alpha$ , respectively. The radial line to a typical beam point is inclined at angle  $\theta$  with that of left end. Also shown in Figure 1(a) are positive direction of vertical displacement  $v$ , positive directions of rotation  $\psi$  and  $\beta$  of cross-section due to the bending moment and shear force, respectively, and positive direction of angle of twist  $\phi$ . The area, area moment of inertia and torsional constant of cross-section at  $\theta$  are denoted as  $A$ ,  $I$  and  $J$ , respectively. Those of cross-section at left end ( $\theta=0$ ) and right end ( $\theta=\alpha$ ) are denoted as  $A_1$ ,  $I_1$  and  $J_1$ , respectively. Also those of cross-section at mid span ( $\theta=\alpha/2$ ) are denoted as  $A_0$ ,  $I_0$  and  $J_0$ , respectively.

The quantities  $A$ ,  $I$  and  $J$  are expressed in the form

$$A = A_1 f \tag{1}$$

$$I = I_1 g \tag{2}$$

$$J = J_1 h \tag{3}$$

where  $f=f(\theta)$ ,  $g=g(\theta)$  and  $h=h(\theta)$  are the functions of the single variable  $\theta$ , as discussed in section SHAPE FUNCTIONS.

A small element of the curved beam with the opening angle  $d\theta$  and arc length  $ds$  shown in Figure 1(b) defines the positive directions for the shear force  $Q$ , the bending moment  $M$ , the torsional moment  $T$ , the vertical inertia force  $F_v$  and the rotatory inertia couple  $C_\phi$ . With the inertia force and the rotatory inertia couple treated as equivalent static quantities, the three equations for dynamic equilibrium of element are

$$\frac{dQ}{d\theta} - aF_v = 0 \tag{4}$$

$$\frac{dM}{d\theta} - aQ + T + aC_\phi = 0 \tag{5}$$

$$M - \frac{dT}{d\theta} = 0 \tag{6}$$

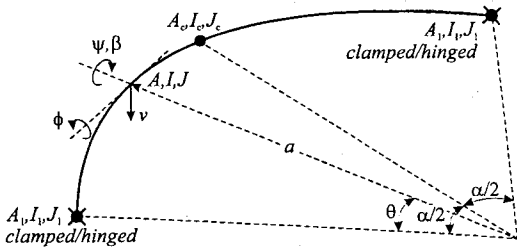


Fig. 1 (a) Geometry of curved beam

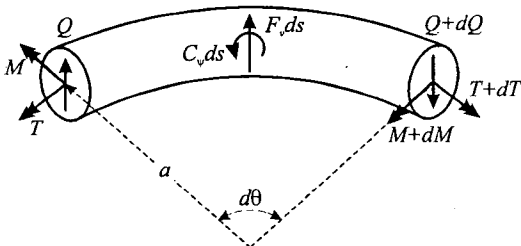


Fig. 1 (b) Loads on a curved beam element

The equations that relate  $M$  and  $T$  to the rotations  $\psi$  and  $\phi$  are as follows<sup>15)</sup>.

$$M = \frac{EI}{a} \left( \phi - \frac{d\psi}{d\theta} \right) = \frac{EI_g}{a} \left( \phi - \frac{d\psi}{d\theta} \right) \tag{7}$$

$$T = \frac{GJ}{a} \left( \psi + \frac{d\phi}{d\theta} \right) = \frac{GJ_h}{a} \left( \psi + \frac{d\phi}{d\theta} \right) \tag{8}$$

where  $E$  and  $G$  are the Young's modulus and shear modulus, respectively.

The total angle between the deformed and undeformed cross-section of the beam is:

$$\frac{dv}{ds} = \frac{1}{a} \frac{dv}{d\theta} = \psi + \beta \tag{9}$$

The transverse shear force  $Q$ , whose effect on the structural behavior is known as the effect of shear deformation, is given by<sup>16)</sup>

$$Q = k\beta GA = kGA_1 f \left( \frac{1}{a} \frac{dv}{d\theta} - \psi \right) \tag{10}$$

where  $k$  is the cross-sectional shape factor. For example, the  $k$  values for a rectangular and a circular section are  $2/3$  and  $3/4$ , respectively.

The beam is assumed to be in harmonic motion, or each co-ordinate is proportional to  $\sin(\omega t)$  where  $\omega$  is the frequency parameter and  $t$  is time. The inertia loadings per unit arc length are then

$$F_v = -dA\omega^2 v = -dA_1 f \omega^2 v \tag{11}$$

$$C_\phi = -dIa\omega^2 \phi = -dI_1 g a \omega^2 \phi \tag{12}$$

where  $d$  is mass density of beam material. The  $C_\phi$  term of equation (12) is known as the effect of rotatory inertia in free vibrations.

When Eqs. (7), (8) and (10) are differentiated once, the results are

$$\begin{aligned} \frac{dM}{d\theta} &= \frac{EI_1}{a} \frac{dg}{d\theta} \left( \phi - \frac{d\psi}{d\theta} \right) \\ &+ \frac{EI_1 g}{a} \left( \frac{d\phi}{d\theta} - \frac{d^2\psi}{d\theta^2} \right) \end{aligned} \quad (13)$$

$$\begin{aligned} \frac{dT}{d\theta} &= \frac{GJ_1}{a} \frac{dh}{d\theta} \left( \psi + \frac{d\phi}{d\theta} \right) \\ &+ \frac{GJ_1 h}{a} \left( \frac{d\psi}{d\theta} + \frac{d^2\phi}{d\theta^2} \right) \end{aligned} \quad (14)$$

$$\begin{aligned} \frac{dQ}{d\theta} &= kGA_1 \frac{df}{d\theta} \left( \frac{1}{a} \frac{dv}{d\theta} - \psi \right) \\ &+ kGA_1 f \left( \frac{1}{a} \frac{d^2v}{d\theta^2} - \frac{d\psi}{d\theta} \right) \end{aligned} \quad (15)$$

To facilitate the numerical studies, the following non-dimensional system parameters are defined. The vertical displacement  $v$  is normalized by the curved beam radius  $a$ :

$$\eta = \frac{v}{a} \quad (16)$$

The slenderness ratio  $\lambda$  is

$$\lambda = \frac{a}{\sqrt{I_1/A_1}} \quad (17)$$

The shear parameter  $\gamma$  and stiffness parameter  $\varepsilon$  are, respectively,

$$\gamma = \frac{kG}{E} \quad (18)$$

$$\varepsilon = \frac{GJ_1}{EI_1} \quad (19)$$

When equations (11) and (15) are substituted into equation (4) and the non-dimensional forms of equations (16)-(19) are used, the result is

$$\begin{aligned} \frac{d^2\eta}{d\theta^2} &= -\frac{1}{f} \frac{df}{d\theta} \frac{d\eta}{d\theta} - \frac{p_i^2}{\gamma\lambda^2} \eta \\ &+ \frac{d\psi}{d\theta} + \frac{1}{f} \frac{df}{d\theta} \psi \end{aligned} \quad (20)$$

When equations (8), (10), (12) and (13) are substituted into equation (5) and the non-dimensional forms of equations (16)-(19) are used, the result is

$$\begin{aligned} \frac{d^2\phi}{d\theta^2} &= -\gamma\lambda^2 \frac{f}{g} \frac{d\eta}{d\theta} - \frac{1}{g} \frac{dg}{d\theta} \frac{d\phi}{d\theta} \\ &+ \left( \gamma\lambda^2 \frac{f}{g} + \varepsilon \frac{h}{g} - \frac{p_i^2}{\lambda^2} \right) \phi \\ &+ \left( 1 + \varepsilon \frac{h}{g} \right) \frac{d\psi}{d\theta} + \frac{1}{g} \frac{dg}{d\theta} \psi \end{aligned} \quad (21)$$

When equations (7) and (14) are substituted into equation (6) and the non-dimensional forms of equations (16)-(19) are used, the result is

$$\begin{aligned} \frac{d^2\phi}{d\theta^2} &= -\left( 1 + \frac{g}{\varepsilon h} \right) \frac{d\psi}{d\theta} \\ &- \frac{1}{h} \frac{dh}{d\theta} \left( \psi + \frac{d\phi}{d\theta} \right) + \frac{1}{\varepsilon} \frac{g}{h} \phi \end{aligned} \quad (22)$$

In last two equations (20) and (21), the  $p_i$  is the non-dimensional frequency parameter defined as

$$p_i = \omega_i a^2 \sqrt{\frac{dA_1}{EI_1}} \quad (23)$$

which is written in terms of  $i$ th frequency  $\omega = \omega_i$ ,  $i=1, 2, 3, 4, \dots$ .

For the curved beam with both clamped ends, the boundary conditions at ends  $\theta=0$  and  $\theta=a$  are

$$\eta=0 \quad (24)$$

$$\frac{d\eta}{d\theta} = 0 \quad (25)$$

$$\phi = 0 \quad (26)$$

For the curved beam with both hinged ends, the boundary conditions at ends  $\theta=0$  and  $\theta=\alpha$  are

$$\eta = 0 \quad (27)$$

$$\frac{d\psi}{d\theta} = 0 \quad (28)$$

$$\phi = 0 \quad (29)$$

The vibration mode is either symmetric or anti-symmetric when the structure is symmetric about its mid span. For the symmetric mode, the boundary conditions at the mid span  $\theta=\alpha/2$  are

$$\frac{d\eta}{d\theta} = 0 \quad (30)$$

$$\psi = 0 \quad (31)$$

$$\frac{d\phi}{d\theta} = 0 \quad (32)$$

For the anti-symmetric mode, the boundary conditions at the mid span  $\theta=\alpha/2$  are

$$\eta = 0 \quad (33)$$

$$\frac{d\psi}{d\theta} = 0 \quad (34)$$

$$\phi = 0 \quad (35)$$

Stress resultants of curved beam may be computed from the following non-dimensional

forms for the bending moment  $M$ , the torsional moment  $T$ , and the transverse shear force  $Q$ . The respective results, obtained from equations (7), (8) and (10) using equations (1)-(3) and (16), are :

$$m = \frac{Ma}{EI_1} = g \left( \phi - \frac{d\psi}{d\theta} \right) \quad (36)$$

$$t = \frac{Ta}{GJ_1} = h \left( \psi + \frac{d\phi}{d\theta} \right) \quad (37)$$

$$q = \frac{Q}{kGA_1} = f \left( \frac{d\eta}{d\theta} - \psi \right) \quad (38)$$

### 3. SHAPE FUNCTIONS : $f$ , $g$ and $h$

The shape functions  $f$ ,  $g$  and  $h$  first introduced in equations (1), (2) and (3), and contained in the governing differential equations (20), (21) and (22), are now defined. The cross-section considered in this study is limited only circular one. Figure 2 shows the diameters of circular cross-section in which  $D$ ,  $D_1$  and  $D_c$  are the diameters at  $\theta$ , at the left end ( $\theta=0$ ) and at the mid span ( $\theta=\alpha/2$ ), respectively.

The linear taper of variable cross-section whose diameter of cross-section varies in accordance with the following equation is chosen as the curved beam member.

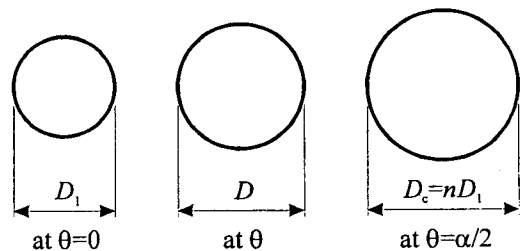


Fig. 2 Diameters of variable circular cross-section

$$D = D_1 \left( \frac{n-1}{\alpha/2} \theta + 1 \right) \quad (39)$$

where  $n$  is the section ratio defined as

$$n = \frac{D_c}{D_1} \quad (40)$$

Using equation (39) gives the properties  $A$ ,  $I$  and  $J$  of circular cross-section at  $\theta$  and the results are

$$A = \frac{\pi D^2}{4} = \frac{\pi D_1^2}{4} (b\theta + 1)^2 = A_1 (b\theta + 1)^2 \quad (41)$$

$$I = I_1 (b\theta + 1)^4 \quad (42)$$

$$J = J_1 (b\theta + 1)^4 \quad (43)$$

where,

$$b = \frac{n-1}{\alpha/2} \quad (44)$$

With equations (1) and (41), with equations (2) and (42), and with equations (3) and (43),  $f$ ,  $g$  and  $h$  are expressed in terms of single variable  $\theta$  as

$$f = (b\theta + 1)^2 \quad (45)$$

$$g = h = (b\theta + 1)^4 \quad (46)$$

When equations (45) and (46) are differentiated once, the results are

$$\frac{df}{d\theta} = 2b(b\theta + 1) \quad (47)$$

$$\frac{dg}{d\theta} = \frac{dh}{d\theta} = 4b(b\theta + 1)^3 \quad (48)$$

#### 4. NUMERICAL METHOD

Based on the above analysis, a general FORTRAN computer program was written to calculate  $p_i$ ,  $\eta = \eta_i(\theta)$ ,  $\psi = \psi_i(\theta)$ ,  $\phi = \phi_i(\theta)$ ,  $m = m_i(\theta)$ ,  $t = t_i(\theta)$  and  $q = q_i(\theta)$ . The numerical method described by Lee and Wilson<sup>2)</sup> was used to solve the differential equations (20)-(22), subjected to the end constraint equations (24)-(26) or (27)-(29). The curved beams with both clamped ends and both hinged ends were considered for the linear tapers with circular cross-section, for given parameters  $\alpha, \lambda, \gamma, \epsilon$  and  $n$ . First, the Runge-Kutta method was used to integrate the differential equations; and then the Determinant Search method was used to calculate the characteristic values  $p_i$ . For the sake of completeness, this numerical procedure is summarized as follows.

1) Specify the curved beam geometry ( $\alpha, \lambda, \gamma, \epsilon, n$ ), and set of three homogeneous boundary conditions which are equations (24)-(26) or (27)-(29).

2) Consider sixth order system, equations (20)-(22), as three initial value problems whose initial values are the three homogeneous boundary conditions  $\theta=0$ , as chosen in step 1. Then assume a trial frequency parameter  $p_i$  in which the first trial value is zero.

3) With the numerical integration technique in which the Runge-Kutta method<sup>17)</sup> was used, integrate equations (20)-(22) from  $\theta=0$  to  $\alpha/2$ . Perform three separate integrations, one for each of the three boundary conditions.

4) From the Runge-Kutta solution, evaluate at mid span ( $\theta=\alpha/2$ ) the determinant  $D$  of the coefficient matrix for the boundary conditions of equations either (30)-(32) for symmetric mode or (33)-(35) for anti-symmetric mode. If  $D=0$ , then the trial value of  $p_i$  is an

eigenvalue. If not, then increment  $p_i$  and repeat above calculations.

5) Repeat steps 3 and 4 and note the sign of  $D$  in each iteration. If  $D$  changes between two consecutive trials, then the eigenvalue lies between these last two trial values of  $p_i$ .

6) Use the Regula-Falsi method<sup>18)</sup>, one of the bracketing methods, to compute the advanced trial  $p_i$  based on its two previous values.

7) Terminate the calculations and print the value of  $p_i$  and mode shapes when the convergence criteria are met.

## 5. COMPUTED RESULTS AND DISCUSSION

In this study, the shear parameter  $\gamma$  and stiffness parameter  $\epsilon$  were chosen as 0.29 and 0.77, respectively, since the cross-section was circular with  $k=3/4$  and  $J_1=2I_1$ , and the material was assumed to be steel with  $G/E=0.385$ . The four lowest values of  $p_i$  which consists of two symmetric and two anti-symmetric modes, and their corresponding mode shapes were calculated.

For numerical examples, suitable convergence of solutions was obtained for an increment of  $\Delta\theta=(\alpha/2)/50$  in Runge-Kutta method referred on the Figure 3 in which the convergence analysis is shown. The convergence criterion was that  $p_i$  solutions obtained with the  $(\alpha/2)/50$  increment agreed with those obtained with the  $(\alpha/2)/100$  increment to within three significant figures.

For the comparison purposes, the finite element solutions based on the commercial package ADINA were used to compute the frequency parameters  $p_i$  and experiments on the laboratory scale curved beam model were done. The experimental setup and methods of

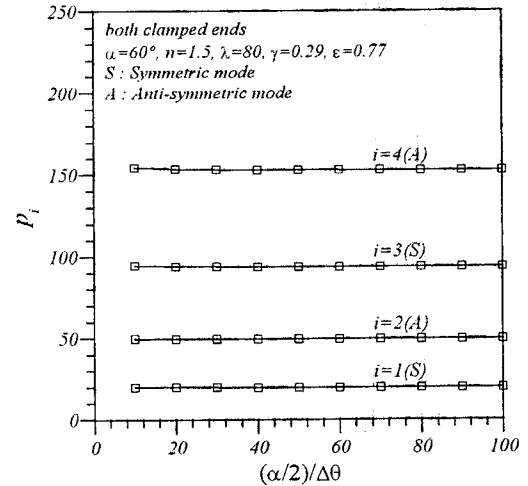


Fig. 3 Convergence analysis

measuring the free vibration frequencies of curved beams are fully described by Lee and Wilson<sup>2)</sup>, and Mo<sup>19)</sup>. For further experimental methods, the reader is referred to these references. The results are shown in Table 1 in which the frequencies of this study agree closely with those of ADINA with the shear areas associated with the transverse shear loadings within a tolerance of 2%. And the measured frequencies averaged about 5.4% less than those predicted from theory. These comparisons serve to validate the numerical method developed herein.

It is shown in Figure 4, for which both clamped ends and both hinged ends with  $\alpha=60^\circ$ ,  $\lambda=80$ ,  $\gamma=0.29$ ,  $\epsilon=0.77$  that the frequency parameters  $p_i$  increase as the section ratio  $n$  increases to 3 except the first mode of both clamped ends. It is observed that the increasing rate of  $p_i$  vs.  $n$  curves is higher at higher mode. Particularly, the increasing rate of first mode is negligible.

It is shown in Figure 5, for which both clamped and both hinged beams with  $\alpha=60^\circ$ ,

Table 1 Comparison of frequency parameters  $p_i$  between this study, ADINA and experiment ( $\alpha=60^\circ, n=0.7, \lambda=80, \gamma=0.29, \epsilon=0.77$ )

End constraints	$i$	Frequency parameter, $p_i$			Deviation (%)	
		this study (A)	ADINA (B)	experiment (C)	$ B-A /A$	$ C-A /A$
both clamped ends	1	20.01 (S) *	19.69	19.38	1.60	3.15
	2	49.02 (A)	48.97	46.77	0.10	4.59
	3	91.98 (S)	91.61	87.20	0.40	5.20
	4	147.9 (A)	147.3	-	0.41	-
both hinged ends	1	5.770 (S) *	5.896	5.460	2.18	5.37
	2	28.20 (A)	28.50	26.10	1.06	7.45
	3	65.45 (S)	65.62	61.01	0.26	6.78
	4	117.6 (A)	116.3	-	1.11	-

\* S : symmetric mode A : anti-symmetric mode

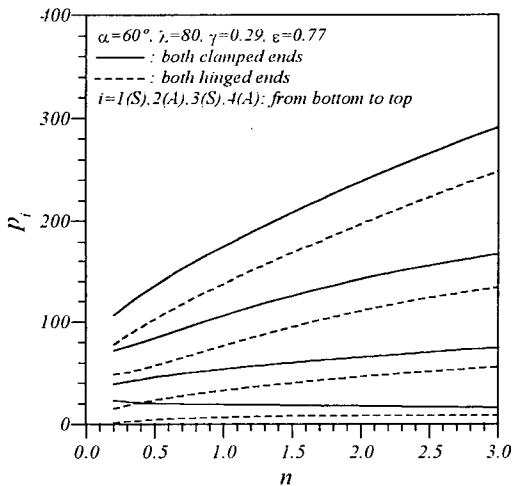


Fig. 4  $p_i$  versus  $n$  curves

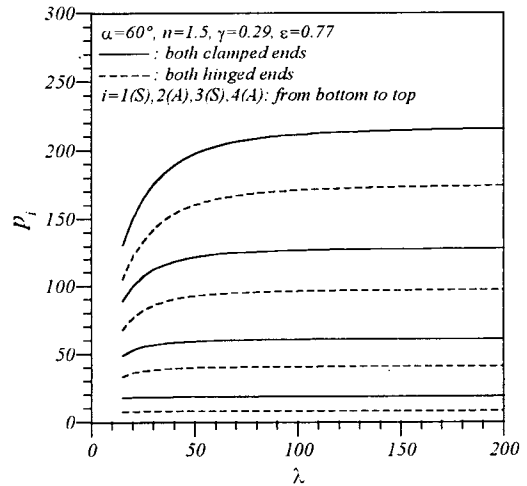


Fig. 5  $p_i$  versus  $\lambda$  curves

$n=1.5, \gamma=0.29, \epsilon=0.77$ , that the  $p_i$  values increase and approach upper limits or horizontal asymptotes as the slenderness ratio  $\lambda$  increases to 200. It is noted that in case of the first modes, the effect of  $\lambda$  on  $p_i$  is negligible.

In Figure 6, both clamped ends, both hinged ends,  $n=1.5, \lambda=80, \gamma=0.29, \epsilon=0.77$ , and the  $p_i$  values all decreases very rapidly opening angle  $\alpha$  increases from  $0^\circ$  to  $90^\circ$ . And it is true that the  $p_i$  values approach lower limits

or horizontal asymptotes as  $\alpha$  increases to  $180^\circ$ .

Typical mode shapes of displacements for symmetric and anti-symmetric are shown in Figure 7, based on both clamped ends,  $\alpha=60^\circ, n=0.7, \lambda=80, \gamma=0.29$  and  $\epsilon=0.77$ . Also shown in this figure are the stress resultant mode shapes for the moment  $m$ , for the torsional moment  $t$ , and for the transverse shear force  $q$ . From this figure and also from Fig-



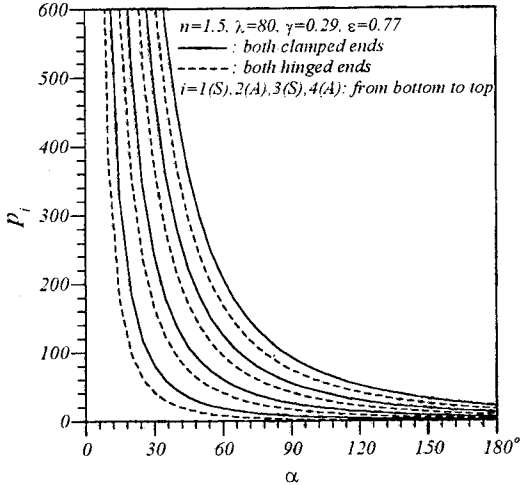


Fig. 6  $p_i$  versus  $\alpha$  curves

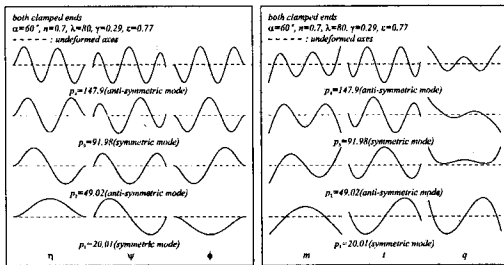


Fig. 7 Mode shapes of displacements and stress resultants

ures 3-6, it is concluded that the odd modes ( $i=1,3$ ) and even modes ( $i=2,4$ ) are symmetric and anti-symmetric, respectively.

6. CONCLUSIONS

The method presented here for calculating frequencies and mode shapes for circular horizontally curved beams of variable cross-section were found to be efficient and reliable over a wide range of system parameters. Governing differential equations for free vibration of such curved beam were derived and solved numerically. The Runge-Kutta method and the

Regula-Falsi method were used to integrate the differential equations and to calculate the frequencies, respectively. Computations showed that the frequencies obtained by present study, ADINA and experiments agreed closely. The lowest four natural frequencies are presented as functions of three non-dimensional system parameters: (1) section ratio, (2) slenderness ratio and (3) opening angle. Typical mode shapes of displacements and stress resultants are presented.

ACKNOWLEDGEMENT

This paper was supported by NON-DIRECTED RESEARCH FUND, Korea Research Foundation in 1996. The authors thank for this financial support.

REFERENCES

1. T. M. Wang, R. H. Nettleton and B. Keita, "Natural Frequencies for Out of Plane Vibrations of Continuous Curved Beams", *Journal of Sound and Vibration*, Vol. 68, No. 3, 1980, pp.427~436.
2. B. K. Lee and J. F. Wilson, "Free Vibrations of Arches with Variable Curvature", *Journal of Sound and Vibration*, Vol. 36, No. 1, 1990, pp.75~89.
3. R. R. Archer, "Small Vibrations of Thin Incomplete Circular Rings", *International Journal of Mechanical Science*, Vol. 1, 1960, pp.45~46.
4. L. S. D. Morley, "The Flexural Vibrations of a Cut Thin Ring", *Quarterly Journal of Mechanics and Applied Math.*, Vol. 11, 1934, pp.429~449.
5. T. V. Ojalvo, "Coupled Twist-Bending Vibrations of Incomplete Elastic Rings", *Inte-*

- International Journal of Mechanical Science*, Vol. 4, 1972, pp.53~72.
6. J. P. Den Hartog, "The Lowest Natural Frequency of Circular Arc", *Philosophical Magazine*, Series 7, Vol. 5, 1928, pp.400~408.
  7. E. Volterra and J.D. Morell, "A Note on the Lowest Natural Frequency of Elastic Arcs", *Journal of the Applied Mechanics*, ASME, Vol. 27, 1960, pp.744~746.
  8. F. C. Nelson, "In-Plane Free Vibration of a Simply Supported Circular Ring Segment", *International Journal of Mechanical Science*, Vol. 4, 1962, pp.517~527.
  9. T. M. Wang and J. M. Lee, "Natural Frequencies of Multi-span Circular Curved Frames", *International Journal of Solids and Structures*, Vol. 8, 1972, pp.791~805.
  10. H. Yonezawa, "Moments and Free Vibrations in Curved Girder Bridges", *Journal of the Engineering Mechanics Division*, ASCE, No. EM1, 1962, pp.1~22.
  11. C. P. Tan and S. Shore, "Dynamic Response of a Horizontally Curved Bridge", *Journal of the Structural Division*, ASCE, Vol. 94, No. ST3, 1968, pp.761~781.
  12. S. S. Rao and V. Sundararajan, "In-Plane Flexural Vibrations of Circular Rings", *Journal of Applied Mechanics*, ASME, Vol. 36, 1969, pp.620~625.
  13. L. L. Philipson, "On the Role of Extension in the Flexural Vibration of Rings", *Journal of Applied Mechanics*, Transactions ASME, Vol.23, 1956, pp.864.
  14. B. S. Seidel and E. A. Erdelyi, "On the Vibration of a Thick Ring in its Own Plane", *Journal of Engineering for Industry*, Transactions ASME, Series B, Vol. 86, 1964, pp.240~244.
  15. E. Volterra and J. H. Gaines, *Advanced Strength of Materials*, Prentice-Hall Inc., 1971.
  16. J. M. Gere and S. P. Timoshenko, *Mechanics of Materials*, 2nd Edition, Brooks/Cole Engineering Division, 1984.
  17. B. Carnahan, H. A. Luther and J. O. Wilkes, *Applied Numerical Methods*, John Wiley & Sons, 1969.
  18. J. H. Ferziger, *Numerical Method for Engineering Application*, John Wiley & Sons, 1981.
  19. J. M. Mo, *A Study on Free Vibrations of Horizontally Curved Beams with Variable Curvature*, Ph. D. Thesis, Wonkwang University, 1998.

(접수일자 : 1998. 1. 17)